

## Raman Thermometry Measurements of Free Evaporation from Liquid Water Droplets

Jared D. Smith,<sup>†,‡</sup> Christopher D. Cappa,<sup>†,‡,§</sup> Walter S. Drisdell,<sup>†,‡</sup>  
Ronald C. Cohen,<sup>†</sup> and Richard J. Saykally<sup>\*,†,‡</sup>

Contribution from the Department of Chemistry, University of California, Berkeley, California 94720, and Chemical Sciences Divisions, Lawrence Berkeley National Laboratory, Berkeley, California 94720

Received May 22, 2006; E-mail: saykally@berkeley.edu

**Abstract:** Recent theoretical and experimental studies of evaporation have suggested that on average, molecules in the higher-energy tail of the Boltzmann distribution are more readily transferred into the vapor during evaporation. To test these conclusions, the evaporative cooling rates of a droplet train of liquid water injected into vacuum have been studied via Raman thermometry. The resulting cooling rates are fit to an evaporative cooling model based on Knudsen's maximum rate of evaporation, in which we explicitly account for surface cooling. We have determined that the value of the evaporation coefficient ( $\gamma_e$ ) of liquid water is  $0.62 \pm 0.09$ , confirming that a rate-limiting barrier impedes the evaporation rate. Such insight will facilitate the formulation of a microscopic mechanism for the evaporation of liquid water.

### Introduction

Interphase mass transfer at the liquid–vapor interface of water is a fundamental process that impacts many areas of physical science, engineering, and biology. However, despite intensive research, the underlying mechanisms and rates of evaporation and condensation remain poorly understood. Recent measurements of the temperature profile across the surface of a rapidly evaporating liquid–vapor interface exhibited a discontinuous temperature increase, wherein the vapor directly above the surface was as much as  $\sim 7^\circ$  warmer than the liquid surface itself. These measurements were interpreted as indicating that molecules in the high-energy tail of the Boltzmann distribution are those most often evaporating.<sup>1</sup> Molecular dynamics (MD) simulations have also shown that the evaporating water molecules exhibit a non-Maxwellian distribution characterized by increased translational energies.<sup>2</sup> Such a conclusion is in contrast to the classical kinetic picture of evaporation, wherein it is assumed that the temperature of the vapor is less than or equal to that of the surface.<sup>1,3</sup> In fact, an elevated vapor temperature suggests there exists an energetic barrier to evaporation in excess of the enthalpy of vaporization. More recent results by Cappa et al. have shown that the relative evaporation rates of light and heavy isotopes of water are strongly composition dependent, which also evidences a barrier to the evaporation process.<sup>4</sup>

The standard kinetic theory of evaporation was first derived by Hertz from analysis of the evaporation of mercury<sup>5</sup> and was later verified by Knudsen.<sup>6</sup> Under equilibrium conditions, the rate of evaporation is equal to the rate of condensation, as there is no net mass transfer between phases. The maximum rate of condensation ( $J_{c,\max}$ ) or evaporation ( $J_{e,\max}$ ) is then the number of molecular collisions per unit time per unit area with the liquid surface, as given by the Knudsen equation<sup>7</sup>

$$J_{c,\max} = J_{e,\max} = \frac{P_0}{\sqrt{2\pi mk_B T}} \quad (1)$$

where  $P_0$  is the equilibrium vapor pressure,  $T$  is the liquid temperature,  $k_B$  is Boltzmann's constant, and  $m$  is the molecular mass. The parameter most often reported in evaporation studies is the evaporation coefficient ( $\gamma_e$ ). The evaporation coefficient is the ratio of the observed rate to that given by the theoretical maximum (eq 1),<sup>8,9</sup> such that

$$J_{c,\text{obs}} = \gamma_e J_{e,\max} = \frac{\gamma_e P_0}{\sqrt{2\pi mk_B T}} \quad (2)$$

where  $J_{e,\text{obs}}$  is the observed evaporation rate. Hence, an evaporation coefficient of unity implies the maximum possible evaporation rate. An evaporation coefficient less than unity indicates that there exists a barrier (energetic or entropic) that limits the rate of evaporation.

<sup>†</sup> University of California.

<sup>‡</sup> Lawrence Berkeley National Laboratory.

<sup>§</sup> Present address: NOAA Earth System Research Laboratory, Chemical Sciences Division and the Cooperative Institute for Research in Environmental Sciences, University of Colorado, Boulder, CO.

(1) Fang, G.; Ward, C. A. *Phys. Rev. E: Stat. Phys., Plasmas, Fluids, Relat. Interdiscip. Top.* **1999**, *59*, 417.  
(2) Tsuruta, T.; Nagayama, G. *J. Phys. Chem. B* **2004**, *108*, 1736.  
(3) Cercignani, C.; Fiszdon, W.; Fressotti, A. *Phys. Fluids* **1985**, *28*, 3237.  
(4) Cappa, C. D.; Drisdell, W. S.; Smith, J. D.; Saykally, R. J.; Cohen, R. C. *J. Phys. Chem. B* **2005**, *109*, 24391.

(5) Hertz, H. *Ann. Phys.* **1882**, *17*, 177.

(6) Knudsen, M. *Ann. Phys.* **1915**, *47*, 697.

(7) Knudsen, M. *The Kinetic Theory of Gases*; Methuen: London, 1950.

(8) Barrett, J.; Clement, C. *J. Colloid Interface Sci.* **1991**, *150*, 352.

(9) Eames, I. W.; Marr, N. J.; Sabir, H. *Int. J. Heat Mass Transfer* **1997**, *40*, 2963.

The evaporation rate of liquid water has been studied for decades; however, measurements have yielded conflicting values for the evaporation coefficient that range over 3 orders of magnitude.<sup>9,10</sup> Furthermore, the degree of deviation from the maximum evaporation rate has been found to depend on the measurement methodology. In general, experiments utilizing a fast flowing, renewable surface measure  $\gamma_e$  to be greater than  $\sim 0.2$ , whereas measurements on stagnant surfaces yield much smaller values.<sup>8,10</sup> Small values of  $\gamma_e$  measured using stagnant surfaces might be attributed to the presence of surface contaminants. Liquid water is extremely sensitive to surface contamination, and accumulated impurities can significantly impede evaporation.<sup>10</sup> Uncertainties in the evaporating surface temperature may also introduce systematic errors into the measurement of  $\gamma_e$ . For macroscopic systems, evaporation can lead to a temperature gradient from the surface to the bulk caused by the slow rate of heat transfer from the bulk to the interface.<sup>1</sup> Any such gradient can subsequently lead to a large systematic error in the measured evaporation coefficient. Another common problem inherent in many evaporation measurements of volatile liquids is the uncertainty in the pressure and temperature of the vapor directly above the surface, which influences the role of condensation. Volatile liquids like water, under most conditions, evaporate into a backpressure of vapor, which can significantly decrease the observed evaporation rate. When this is the case, eq 1 must be modified to account for condensation to correctly describe the maximum rate. However, the use of this modified equation hinges on having an accurate knowledge of the vapor temperature and pressure directly above the surface, which is often difficult to ascertain.

To transcend the experimental obstacles that have impeded previous measurements of water evaporation rates, we have employed a vibrating orifice aerosol generator (VOAG) to inject a train of small (radius = 6–20  $\mu\text{m}$ ) liquid  $\text{H}_2\text{O}$  droplets into a high vacuum chamber. The problem of surface contamination is largely eliminated by the use of a droplet train due to the fast flowing, constantly renewed surface. In fact, the longest exposure times in these experiments are less than a few milliseconds. We have also developed a model that explicitly characterizes the extent to which any surface-to-bulk temperature gradient is established. The results from this model indicate that the small size of the droplets prevents the establishment of a significant temperature gradient. Furthermore, to the extent that a temperature gradient does exist, it can be quantitatively accounted for. Another major advantage of using small droplets in high vacuum is that the water molecules evaporate ballistically (without collisions). Because the evaporating molecules experience only a negligible number of gas-phase collisions, which could redirect them back toward the droplet, we are able to study free evaporation without the complication of condensation. The increase in evaporation rate from the surface curvature of the droplets (i.e. Kelvin effect) is extremely small ( $<0.02\%$ ) for the droplet sizes employed in these experiments.

The ballistic evaporation condition is easily confirmed by considering the decrease in vapor density ( $n$ ) as a function of distance ( $r$ ) from a droplet of radius ( $r_o$ ) given by

$$n(r) = n(r_o) \frac{r_o^2}{r^2} \quad (3)$$

where  $n(r_o)$  is the vapor density directly above the droplet

surface. The average number of collisions ( $N_{\text{coll}}$ ) experienced by a molecule that has traveled far from the droplet surface is determined by integrating over the radial collision frequency

$$N_{\text{coll}}(r_o, T) = \int_{r_o}^{\infty} \frac{dr}{\lambda(r, T)} = \sqrt{2\pi} \sigma_{\text{coll}}^2 n(r_o) r_o^2 \int_{r_o}^{\infty} \frac{dr}{r^2} = \frac{r_o}{\lambda(r_o, T)} \quad (4)$$

where  $\lambda(r, T) = [\sqrt{2\pi} \sigma_{\text{coll}} n(r)]^{-1}$  is the mean free path of the evaporated water molecules, and  $\sigma_{\text{coll}}$  is the collision diameter for water ( $2.6 \times 10^{-10}$  m).<sup>11</sup> Therefore, when the droplet radius is less than the mean free path of the vapor directly above the surface ( $\lambda(r_o, T)$ ), evaporating molecules experience less than a single collision on average. The equilibrium vapor pressure of water at 283 K, the temperature of the droplets near the VOAG orifice, is approximately 9 Torr, which corresponds to a mean free path of 10  $\mu\text{m}$ . Therefore, if we generate droplets with radii less than 10  $\mu\text{m}$ , most molecules from these droplets will evaporate in a ballistic manner. Faubel et al.<sup>12</sup> have previously measured the velocity distribution of vapor molecules evaporation from cylindrical microjet operating in vacuum. They confirmed that for a 10  $\mu\text{m}$  diameter jet the velocity distribution is indicative of nearly collision free evaporation. The spherical geometry of the droplets used in the measurements presented here ensure that even fewer gas-phase collisions will occur. Furthermore, it should be pointed out that the ballistic evaporation condition is significantly relaxed for our measurements because the majority of collisions that do occur will not reverse the trajectory of the molecule causing it to recondense back on the droplet surface.

In these experiments, the temperature of the rapidly cooling droplets is directly measured using the Raman spectrum as a noninvasive temperature probe.<sup>13,14</sup> Using an extended version of the cooling model developed by Faubel et al.,<sup>15</sup> wherein we explicitly account for surface cooling, we are able to extract the evaporation coefficients for liquid  $\text{H}_2\text{O}$  from the measured temperature changes. We have found that evaporation proceeds at less than the maximum rate ( $\gamma_e = 0.62 \pm 0.09$ ), thereby confirming the existence of a barrier impeding the evaporation process. Furthermore, and in contrast to recent measurements of the condensation coefficient,<sup>16</sup> we have found that the evaporation coefficient has only a weak dependence on temperature.

## Experimental Methods

To examine evaporation from liquid water, we have measured the change in temperature due to evaporative cooling of a droplet train injected into vacuum using a VOAG. The liquid water used in all measurements is deionized and filtered (18.2 M $\Omega$  resistivity Milli-Q, Millipore) with a measured total organic content of 3–4 ppb. The VOAG is comprised of a liquid jet formed by forcing water through a fused silica capillary pulled to a radius of 3–10  $\mu\text{m}$ , and mounted on a piezoelectric ceramic that is modulated with a square wave voltage

- (10) Marek, R.; Straub, J. *Int. J. Heat Mass Transfer* **2000**, *44*, 39.
- (11) Hirschfelder, J. O. *Molecular Theory of Gases and Liquids*; J. Wiley: New York, 1954.
- (12) Faubel, M.; Kisters, T. *Nature* **1989**, *339*, 527.
- (13) Davis, K. L.; Liu, K. K.; Lanan, M.; Morris, M. D. *Anal. Chem.* **1993**, *65*, 293.
- (14) Vehring, R.; Schweiger, G. *Appl. Spectrosc.* **1992**, *46*, 25.
- (15) Faubel, M.; Schlemmer, S.; Toennies, J. P. *At., Mol., Clusters* **1988**, *10*, 269.
- (16) Li, Y. Q.; Davidovits, P.; Shi, Q.; Jayne, J. T.; Kolb, C. E.; Worsnop, D. R. *J. Phys. Chem. A* **2001**, *105*, 10627.

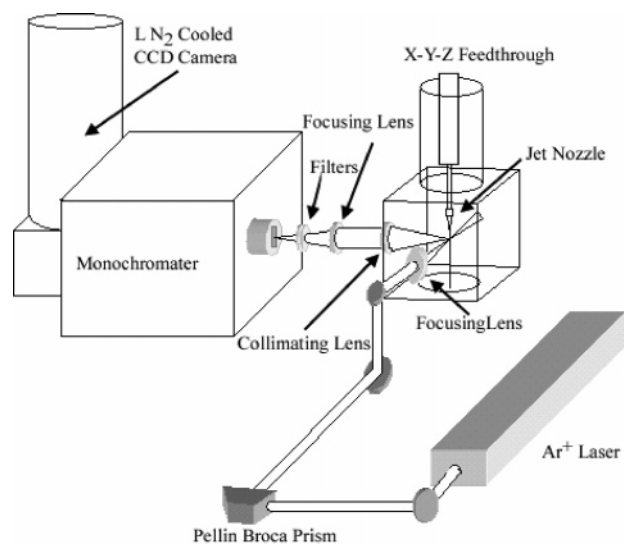


**Figure 1.** Schematic view of experimental apparatus.

from a frequency generator (0–20 V, 100–800 kHz). The modulation produces a collimated train of droplets with a very well-defined size distribution and a dispersion in the radius of less than  $0.1 \mu\text{m}$ <sup>17</sup>. The VOAG is mounted on an X, Y, Z manipulator to the top face of a 7 cm cubical vacuum chamber evacuated by a 110 L/s turbomolecular pump. The VOAG is pressurized by a high-pressure syringe pump, wherein the flow rate can be controlled to within  $\pm 0.5\%$ . The droplet radius ( $r_0$ ) is determined from the liquid flow rate ( $F$ ) and the modulation frequency ( $f$ ) according to

$$r_0 = \left(\frac{3F}{4\pi f}\right)^{1/3} \quad (5)$$

Once the droplets leave the interaction region, they are dumped into a liquid nitrogen trap located 50 cm from the nozzle. The background pressure in the main chamber is less than  $5 \times 10^{-4}$  Torr, which corresponds to a mean free path greater than 50 cm. The vacuum chamber is equipped with viewports, which allow for the introduction of the 514.5 nm line of an  $\text{Ar}^+$  laser operating at  $\sim 250$  mW. The light is focused onto the jet by a 3 mm focal length lens resulting in a  $\sim 40 \mu\text{m}$  diameter spot size. The  $90^\circ$  Raman scattered light is recollimated, filtered, and focused into a fiber optic, which is coupled to a 0.5 m monochromator equipped with a liquid nitrogen cooled CCD camera. A schematic of the experimental apparatus is shown in Figure 1.

It has been previously demonstrated that the position and line shape of the  $-\text{OH}$  Raman spectrum of liquid water are very sensitive to temperature.<sup>18,19</sup> Therefore, it is possible to exploit this sensitivity to measure the temperature of water using the calibrated Raman spectrum.<sup>13,14</sup> Our method of temperature determination has been previously described by Wilson et al.<sup>20</sup> for temperature measurements on liquid microjets and is very similar to experiments described by Vehring and Schweiger<sup>14</sup> for a micron sized droplet chain operating in air. Temperature calibration curves are obtained by collecting the total Raman scattering intensity (both vertical and horizontal polarizations) as a function of temperature over the range of 0–50 °C. The calibration temperature was measured using a thermostated nozzle assembly with a  $100 \mu\text{m}$  diameter orifice operating at atmospheric pressure. By measuring the droplet train temperature, using a small calibrated

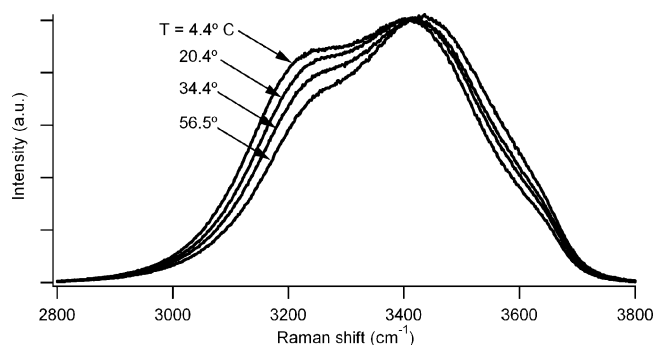


**Figure 2.** Raman spectra of the OH stretching band at selected temperatures used to generate the temperature calibration curve.

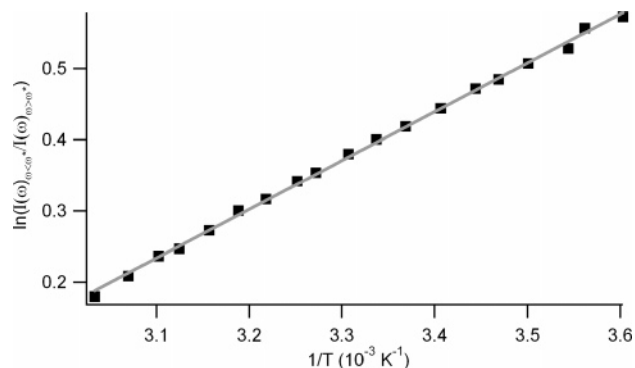


**Figure 3.** Calibration curve used in the determination of the liquid droplet temperature by Raman spectroscopy. The linear fit to the data is shown ( $R^2 = 0.999$ ).

thermocouple, we have found that at atmospheric pressure evaporative cooling is minimal. The resulting spectra were baseline corrected and intensity normalized. Examples of Raman spectra taken on the calibration droplet train are shown in Figure 2. The spectra were then integrated from the low-frequency baseline to an arbitrary point near the center of the spectrum ( $\omega^*$ ), and then from  $\omega^*$  to the high-frequency baseline. The calibration curve was constructed by plotting the natural logarithm of the ratios of integrated band areas vs inverse temperature, as shown in Figure 3. Such a plot will always produce a straight line independent of the choice of  $\omega^*$ , and it is therefore only necessary to be consistent in the choice of  $\omega^*$ .<sup>21</sup> Using this calibration curve, we can determine the temperature, to  $\pm 2^\circ$ , at specific points along the axis of propagation of the droplet train. Data is collected over the range of 245–295 K which requires an extrapolation of our calibration curve to lower temperatures. However, It has been shown that this type of van't Hoff plot is very linear over a relatively large temperature range ( $\sim 100^\circ$ ),<sup>21,22</sup> and therefore, our extrapolation will most likely not introduce significant error. The distance away from the nozzle was measured with a micrometer to within  $\pm 0.01$  mm. Distance is converted into vacuum interaction time from the jet velocity ( $v_{\text{jet}} = F/\pi r_{\text{jet}}^2$ ), where  $r_{\text{jet}}$  is the radius of the capillary (as opposed to the radius of the droplets). The radius of the capillary is determined by forcing water through the capillary with the frequency generator turned off which allows for the formation of a cylindrical liquid jet. We are then able to measure the size of the jet (which is the same as capillary orifice) to  $\pm 0.05 \mu\text{m}$  using the angular dependent Mie scattering intensity as previously described by Cappa et al.<sup>4</sup> The initial jet temperature (at  $t = 0$ ) is determined by measuring the temperature of the droplet train at atmospheric pressure wherein evaporative cooling is negligible.

A potential complication with our measurement is that the droplets have only a limited amount of space between them. Therefore, some

(17) Sayer, R. M.; Gatherer, R. D. B.; Gilham, R. J. J.; Reid, J. P. *Phys. Chem. Chem. Phys.* **2003**, *5*, 3732.

(18) Walrafen, G. E.; Hokmabadi, M. S.; Yang, W.-H. *J. Chem. Phys.* **1986**, *85*, 6964.

(19) D'Arrigo, G.; Maisano, G.; Mallamace, F.; Migliardo, P.; Wanderlingh, F. *J. Chem. Phys.* **1981**, *75*, 4264.

(20) Wilson, K. R.; Rude, B. S.; Smith, J.; Cappa, C.; Co, D. T.; Schaller, R. D.; Larsson, M.; Catalano, T.; Saykally, R. *J. Rev. Sci. Instrum.* **2004**, *75*, 725.

(21) Smith, J. D.; Cappa, C. D.; Wilson, K. R.; Cohen, R. C.; Geissler, P. L.; Saykally, R. J. *Proc. Natl. Acad. Sci. U.S.A.* **2005**, *102*, 14171.

(22) Geissler, P. L. *J. Am. Chem. Soc.* **2005**, *127*, 14930.

fraction of the evaporating molecules will recondense on neighboring droplets. In the measurements reported here the average spacing between adjacent droplet centers is  $6r_o$ . Because the droplets are injected into vacuum they should only experience minimal drag from the vapor. Therefore, we expect that the droplet velocities will remain relatively constant, and thus the spacing between droplets should remain constant over the time scale of our measurements. To calculate the fraction of evaporating molecules which will condense on adjacent droplets we start by calculating the flux ( $\Phi$ ) of molecule at a distance  $r$  from a droplet of radius  $r_o$ ;

$$\Phi(r) = \frac{J_e 4\pi r_o^2}{4\pi r^2} = \frac{J_e r_o^2}{(6r_o)^2} = \frac{J_e}{36} \quad (6)$$

Here we have made the substitution  $r = 6r_o$ , the average distance to the adjacent droplet. Therefore, the number of evaporated molecules colliding with the adjacent droplets ( $N_{\text{coll}}$ ) is given by

$$N_{\text{coll}} = 2\Phi(r)\sigma_{\text{drop}} \quad (7)$$

where  $\sigma_{\text{drop}}$  is the cross section of the adjacent droplets [ $\sigma_{\text{drop}} = \pi r_o^2$ ], and the factor of 2 in eq 7 accounts for the fact that there are two droplets adjacent to any given droplet. Finally we can calculate the fraction of evaporating molecules that collide with an adjacent droplet ( $n_{\text{frac}}$ ) using

$$n_{\text{frac}} = \frac{N_{\text{coll}}}{J_e 4\pi r_o^2} = \frac{1}{72} \quad (8)$$

Therefore, only about 1.4% of the evaporating molecules will condense on the adjacent droplets. Thus, recondensation onto neighboring droplets will result in an underestimate in the evaporation coefficient of less than 0.01. However, this calculation assumes that all molecules which collide with the droplet will condense (i.e., that the condensation coefficient is unity) and, therefore, represents a maximum.

## Results and Discussion

A droplet injected into vacuum will quickly evaporate, which leads to rapid cooling of the liquid as the evaporating molecules carry heat away from the droplet. If the droplet is sufficiently small we can model this process using the Hertz–Knudsen evaporation rate  $\gamma_e J_{e,\text{max}}$  (molec/m<sup>2</sup> s), and the ratio of the enthalpy of vaporization,  $\Delta H_{\text{vap}}$  (J/molec) to the constant pressure heat capacity,  $C_p$  (J/molec K). The model used is an extension of the one formulated by Faubel et al.,<sup>15</sup> whereas here we explicitly account for surface cooling which can lead to the formation of a thermal gradient from the bulk to the surface of the droplet. This is accomplished by dividing a model droplet into thin spherical shells of width  $\delta r$ . The outermost shell is allowed to evaporatively cool, and all of the spherical shells below the surface are cooled through heat transfer between the neighboring shells at a rate determined by the calculated thermal gradient and water's thermal conductivity (0.61 W/m K). The change in temperature ( $T$ ) of the droplet surface (i.e., the outer shell) as a result of evaporative cooling is given by

$$\frac{dT}{dt} = -\gamma_e J_{e,\text{max}} A \frac{\Delta H_{\text{vap}}}{C_p M_d} \quad (9)$$

where  $A = 4\pi r_o^2$  is the surface area of the droplet, and  $M_d = 4/3\pi(r_o^3 - r_1^3)\rho_1$  is the mass of the spherical shell of width  $\delta r = r_o - r_1$  ( $\rho_1$  = density). Substitution of eq 2 and the droplet mass

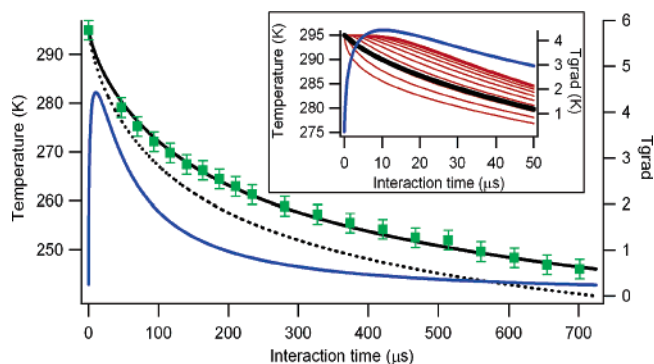


**Figure 4.** Measured temperatures for a 6.5  $\mu\text{m}$  droplet in vacuum (■) compared to the results from the evaporative cooling model wherein the droplet is divided into 100, 65-nm thick, spherical shells. The outer-most shell is allowed to evaporatively cool, and the inner shells cool only by thermal conduction. The solid black line is the volume averaged temperature of all shells fit to the temperature data. The best fit to this data set results in an evaporation coefficient of 0.62 which is compared with the cooling curve for an evaporation coefficient of one (dashed black line). The blue line is a plot of the thermal gradient ( $T_{\text{grad}} = T_{\text{surf}} - T_{\text{avg}}$ ). The inset magnifies the first 50  $\mu\text{s}$  of the model showing the temperature of 10 of the individual spherical shells (red lines), the higher temperature curves are from rings closer to the droplet center.

and surface area into eq 9 gives

$$\frac{dT}{dt} = -\frac{\gamma_e P_0}{\sqrt{2k_B T \pi m}} \frac{\Delta H_{\text{vap}}}{C_p} \frac{3r_o^2}{(r_o^3 - r_1^3)\rho_1} \quad (10)$$

The vapor pressure  $P_0$  is calculated using the empirical equation reported by Murphy and Koop,<sup>23</sup> and  $\rho_1$  is calculated using an equation given by Hare and Sorenson.<sup>24</sup> It was confirmed that taking into account the temperature dependence of the enthalpy of vaporization and the heat capacity has only a negligible effect because their ratio is nearly constant over the entire temperature range studied. It should also be noted that ignoring the temperature dependence of the density (i.e., assuming  $\rho_1 = 1.0$  g/mL), and calculating the vapor pressure from the Clausius–Clapeyron equation [ $P_0 = A \exp(\Delta H_{\text{vap}}/RT)$ ] has only a very minor effect on our model as well.

To model the change in temperature of the droplet as a function of time, we have numerically integrated eq 10. After the initial time step (100 ns) a temperature gradient is established between the outer shell and its neighboring shell. The flow of heat ( $Q$ ) from any shell to its neighboring shell as a result of thermal conduction is then calculated using

$$\frac{dQ}{dt} = -\kappa A \frac{dT}{dr} \quad (11)$$

where  $\kappa$  is the thermal conductivity of water and  $A = 4\pi r_1^2$  is the surface area of the shell. The temperatures of the shells are then calculated at each time step based on the flow of heat in and out of each shell and the specific heat capacity of each shell. Therefore, using both eqs 10 and 11, we can then calculate the volume averaged temperature as a function time. The temperature calculated from our model is then fit to the measured temperature data by varying the evaporation coefficient in eq 10. Figure 4 shows the results of this model fit to the data from 6.5  $\mu\text{m}$  radius droplets. In this model, the droplet

(23) Murphy, D. M.; Koop, T. *J. R. Meteorol. Soc.* **2005**, *131*, 1539.

(24) Hare, D. E.; Sorenson, C. M. *J. Chem. Phys.* **1987**, *87*, 4840.

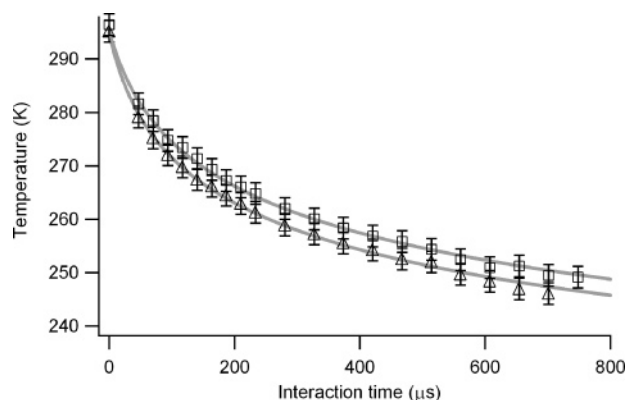


**Figure 5.** Temperature of droplets as a function of vacuum interaction time from two separate experiments where the droplet radius was  $6.5 \mu\text{m}$  ( $\Delta$ ) and a  $7.75 \mu\text{m}$  ( $\square$ ). Data is fit to simple evaporative cooling model, wherein we do not account for surface cooling, with evaporation coefficients of 0.71 and 0.66, respectively.

was divided into 100, 65-nm thick, spherical shells. The temperature of every tenth shell is plotted versus time (see inset), as well as the volume averaged temperature ( $T_{\text{Avg}}$ ), and the temperature gradient ( $T_{\text{Grad}} = T_{\text{Surf}} - T_{\text{Avg}}$ ). Note that the volume averaged temperature corresponds to the temperature measured using the Raman spectrum. At short time ( $t < 20 \text{ s}$ ), a small temperature gradient is established ( $T_{\text{Grad}} \approx 4^\circ$ ). However, as the temperature of the droplet continues to decrease the evaporation rate and  $T_{\text{Grad}}$  correspondingly decrease as the rate of thermal diffusion begins to catch up to the rate of heat loss from the surface layer, and by  $100 \mu\text{s}$   $T_{\text{Grad}}$  is less than  $2^\circ$ . Employing this method on a variety of droplet trains we have found that the best fit to our data results in an evaporation coefficient for  $\text{H}_2\text{O}$  of  $0.62 \pm 0.09$ . The stated error represents twice the standard deviation calculated from measurements on 7 different droplet sizes in the range of  $6\text{--}8 \mu\text{m}$ .

We have also modeled the change in droplet temperature assuming that it is homogeneous throughout the droplet, i.e., that there is no thermal gradient. This is done by not dividing the droplet into spherical shells, and changing  $M_d$  in eq 9 to the mass of the entire droplet (i.e.,  $M_d = 4/3\pi r_o^3 \rho_l$ ). As seen in Figure 5 the quality of the fit to our experimental data is nearly identical for this simple model in which there is no thermal gradient present. However, the evaporation coefficient derived using this model is  $0.71 \pm 0.09$ , which is somewhat higher than the value derived using the surface cooling model, but still within our stated uncertainty. Given that our data are fit well by both models it is difficult to determine whether a temperature gradient actually exists in the droplet. Recent measurements indicate that a 0.5-mm thick isothermal layer exists directly below the liquid water surface as it rapidly evaporated, due to surface-tension driven convection.<sup>25</sup> However, these measurements were performed on a macroscopic system in steady state, and therefore may not be applicable to the measurements presented here. In fact, it is reasonable to assume that, given the rapid cooling rate of our droplets ( $\sim 10^5 \text{ K/s}$ ), convection might be an ineffective method of thermal transport.

We have also performed temperature measurements on larger radius droplets ( $r_o = 9\text{--}20 \mu\text{m}$ ), fits to which result in smaller derived evaporation coefficients. However, it should be clarified

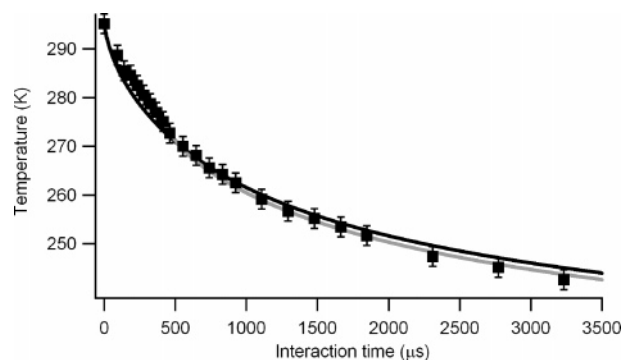


**Figure 6.** Temperature of droplets as a function of vacuum interaction time for droplets with a radius of  $20.3 \mu\text{m}$ . The black curve shows a fit to all of the data, which results in an evaporation coefficient of 0.52, and the gray curve shows a fit to only the low-temperature data ( $\leq 273 \text{ K}$ ), which results in an evaporation coefficient of 0.6. It is expected that the low-temperature data is more reliable because the lower vapor pressure ensures ballistic evaporation.

that the apparent decrease in the evaporation coefficient for these larger droplets simply points out a limitation in our model, and does not imply that the droplets are evaporating at a slower rate. In particular, the evaporating molecules suffer more collisions due to the larger droplet size, and thus there is an increase in the recondensation of evaporating molecules, which is not taken into account by eq 10. Inclusion of these effects in our model would require knowledge of both the vapor density and temperature above the surface. As an example, Figure 6 shows the measured temperature data for a  $20.3 \mu\text{m}$  radius droplet train fit to our evaporative cooling model, which results in an evaporation coefficient of 0.52. However, it is clear that our model does not fit the data very well most likely as a result of the complications just described. We would expect that at lower temperatures the larger droplets will evaporate ballistically (due to the lower vapor pressure), and in fact, on the basis of eq 4, the number of vapor-phase collisions for a 20.3 micron jet will be less than one at temperatures below 273 K. Therefore, we have also fit the data in Figure 6 to our cooling model using only the low-temperature data ( $\leq 273 \text{ K}$ ) which yields an evaporation coefficient of 0.6 which is in very good agreement with our measurements on smaller droplets. We have found that this is the case for all of the measurements performed on larger droplets.

The method we have described so far to determine the evaporation coefficient assumes that it is independent of temperature. The fact that we do not see any significant decrease in the quality of the fit to our model as a function of temperature indicates that this is indeed a reasonable assumption, and strongly indicates that the temperature dependence of the evaporation coefficient must be rather weak. This lack of temperature dependence may indicate that the barrier impeding evaporation is entropic in nature possibly due to geometric requirements for evaporation. As a simple method of exploring the possible temperature dependence of the evaporation coefficient we assume that the barrier is purely energetic, and that the coefficient is exponentially related to the barrier height (i.e.,  $\gamma \approx \exp(E_a/k_B T)$ ). If we incorporate such a temperature dependence into our cooling model we find that the best fit to our data results in an activation barrier of  $1.1 \pm 0.1 \text{ kJ/mol}$  and an evaporation coefficient of  $0.65 \pm 0.08$  at 298 K and  $0.59 \pm 0.08$  at 245 K. However, using a temperature-independent value of 0.62 (the average  $\gamma_e$  over our temperature range), as described

(25) Ward, C. A.; Stanga, D. *Phys. Rev. E: Stat. Phys., Plasmas, Fluids, Relat. Interdiscip. Top.* **2001**, *64*, 1.

above, results in a nearly identical fit to our data. Therefore, although we can rule out a large temperature dependence, we cannot distinguish between an evaporation coefficient with a weak temperature dependence and a evaporation coefficient which is independent of temperature. Therefore, our measurements cannot determine whether the barrier to evaporation is energetic or entropic in nature. However, Faubel et al. have found that the velocity distribution of evaporating water molecules is fit well by an ordinary Maxwellian, indicating that there is no significant energetic barrier to evaporation.<sup>12</sup> Furthermore, the previously mentioned temperature jump across the liquid–vapor interface, measured by Fang and Ward,<sup>1</sup> was only 7°. Such a small increase in temperature would also indicate that any energetic barrier is relatively small. We have also attempted to fit the data using an inverse temperature-dependent evaporation coefficient, and have found that, although a weak increase in the evaporation coefficient (0.58 to 0.64) with decreasing temperature (295 to 245 K) is generally consistent with our data, the quality of the fit is consistently worse compared with a normal temperature dependence.

To summarize, we have found, using a model which incorporate surface cooling, that the evaporation coefficient is either independent of temperature and has a value of  $0.62 \pm 0.09$ , or is weakly temperature dependent and varies between  $0.65 \pm 0.08$  at 298 K and  $0.59 \pm 0.08$  at 245 K. Furthermore, we have also employed a very simple model, which does not allow for a temperature gradient or a temperature dependence to the evaporation coefficient, which results in a value of  $0.71 \pm 0.09$ . These results clearly indicate that a small energetic or entropic barrier impedes the evaporation process. These results are in excellent agreement with a recent measurement of a ballistically evaporating D<sub>2</sub>O ice filament near 273 K in which the evaporation coefficient was found to be  $0.7 \pm 0.3$ , and nearly independent of temperature.<sup>26</sup> It should be pointed out that ice near its melting point is thought to have a highly disordered surface,<sup>26</sup> or possibly even a thin quasi-liquid layer.<sup>27</sup> Therefore, it is not necessarily surprising that the evaporation rate of ice near its melting point is very similar to that of liquid water.

As eq 1 indicates, the rate of evaporation is directly related to the rate of condensation, and therefore, the condensation coefficient,  $\gamma_c$ , (or mass accommodation coefficient) can be defined in an equivalent manner as the evaporation coefficient (i.e.,  $\gamma_e = \gamma_c$ ). As is the case with the evaporation coefficient, considerable discrepancies exist in the reported values of the condensation coefficient.<sup>10</sup> In fact, the two most recent measurements of the condensation coefficient, by Li et al.<sup>16</sup> and Winkler et al.<sup>28</sup> are 0.3 and 1.0, respectively. Li et al. determined the condensation coefficient from measurements of the uptake of isotopically labeled gas-phase water in a droplet train flow reactor.<sup>16</sup> The results of these measurements indicate that the condensation coefficient has an inverse temperature dependence with a value of 0.17 at 280 K which increases to 0.32 at 258 K. Both the absolute value and the relatively strong temperature dependence of the condensation coefficient determined from the uptake measurements are inconsistent with the data reported

here. A computational fluid dynamics study<sup>29</sup> of the droplet train flow reactor experiment has indicated that, due to large uncertainties in the gas-phase resistance, the measurements by Li et al. are actually consistent with a condensation coefficient between 0.2–1.0 at 273 K. If this were the case, it could explain the inconsistency with our measurements, although the validity of this reconsideration has been questioned.<sup>30</sup> In the study by Winkler et al.,<sup>28</sup> condensation of supersaturated water onto nanometer sized silver particles was measured, the results of which indicated that the condensation coefficient for water is in the range of 0.4–1.0 for temperatures between 250 and 290 K. However, it was concluded in this study that the condensation coefficient is most likely one, which is larger than the value for the evaporation coefficient reported here. It was recently suggested by Davidovits et al.<sup>31</sup> that the condensation coefficient reported by Winkler et al. may be an overestimate due to the rapid rate of droplet growth in these experiments. It was proposed that the large flux of vapor molecules at the surface promoted the condensation of surface accommodated species. It was further postulated that a rapidly condensing surface may be highly disordered, which would lead to a large fraction of dangling hydrogen bonds available to interact with incoming molecules.<sup>32</sup> However, it seems very unlikely that condensation would result in a structural perturbation at the molecular level. For instance, based on eq 2 at 298 K and a supersaturation of 1.4, a 10 nm<sup>2</sup> patch of water surface, which is very large compared to the correlation length, will experience only a single collision every 10 ns. However, interfacial molecular fluctuations take place on the picosecond time scale.<sup>33</sup> Therefore, condensation events are extremely rare compared with the timescales of structural rearrangements and should, thus, have little effect on the average molecular orientation.

A number of theoretical studies have used MD simulations to investigate the evaporation and condensation rates of liquid water. However, similar to the experimental measurements, there appears to be conflicting results from different studies. For instance, Yang et al.<sup>34</sup> found that evaporation coefficient for water is less than one and increases with increasing temperature. However, a separate study by Ishiyama et al.<sup>35</sup> indicated that the evaporation coefficient was near unity at room temperature, but decreased significantly with increasing temperature. Similar studies of the condensation coefficient have also indicated that the coefficient decreases with increasing temperature.<sup>2</sup> Given the variation in the results, it appears that MD simulation maybe incapable of providing a quantitatively accurate value for the evaporation coefficient of liquid water.

Much of the interest in the evaporation and condensation of water has been due to the obvious implications in the microphysics of cloud formation. However, if the condensation or evaporation coefficient is relatively large, droplet growth rates in clouds will be diffusion limited in the gas phase, and therefore relatively independent of the coefficient.<sup>31</sup> In fact, simulations

- (26) Sadtchenko, V.; Brindza, M.; Chonde, M.; Palmore, B.; Eom, R. *J. Chem. Phys.* **2004**, *121*, 11980.  
(27) Bluhm, H.; Ogletree, D. F.; Fadley, C. S.; Hussain, Z.; Salmeron, N. *J. Phys. Condens. Mater.* **2002**, *14*, L227.  
(28) Winkler, P. M.; Virtala, A.; Wagner, P. E.; Kulmala, M.; Lehtinen, K. E. J.; Vesala, T. *Phys. Rev. Lett.* **2004**, *93*.

- (29) Morita, A.; Sugiyama, M.; Kameda, H.; Koda, S.; Hanson, D. R. *J. Phys. Chem. B* **2004**, *108*, 9111.  
(30) Davidovits, P.; Worsnop, D. R.; Williams, L. R.; Kolb, C. E.; Gershenzon, M. *J. Phys. Chem. B* **2005**, *109*, 14742.  
(31) Davidovits, P.; Worsnop, D. R.; Jayne, J. T.; Kolb, C. E.; Winkler, P.; Virtala, A.; Wagner, P. E.; Kulmala, M.; Lehtinen, K. E. J.; Vesala, T.; Mozurkewich, M. *Geophys. Res. Lett.* **2004**, *31*.  
(32) Davidovits, P.; Kolb, C. E.; Williams, L. R.; Jayne, J. T.; Worsnop, D. R. *Chem. Rev.* **2006**, *106*, 1323.  
(33) Garrett, B. C.; Schenter, G. K.; Morita, A. *Chem. Rev.* **2006**, *106*, 1355.  
(34) Yang, T. H.; Pan, C. *Int. J. Heat Mass Transfer* **2005**, *48*, 3516.  
(35) Ishiyama, T.; Yano, T.; Fujikawa, S. *Phys. Fluids* **2004**, *16*, 4713.

of droplet growth rates show very little difference between a condensation coefficient of 1.0 and 0.3.<sup>36</sup> In a recent commentary by Laaksonen et al.,<sup>37</sup> they argue that current cloud models are only consistent with available data if the condensation coefficient is near unity. However, they only show results from calculations using a condensation coefficient of 0.1 or 1.0, but it seems likely that a value of  $0.62 \pm 0.09$ , as reported here, would also be consistent with available data. Furthermore, based on the relatively weak temperature dependence we have measured here, it is likely that cloud formation will not be limited by the condensation coefficient at atmospherically relevant temperatures.

### Summary

Temperatures of rapidly evaporating liquid water droplets injected into vacuum have been measured via Raman thermom-

etry. The observed temperatures are fit well by an evaporative cooling model that demonstrates that the evaporation coefficient of water is  $0.62 \pm 0.09$ . Furthermore, we find that the evaporation coefficient has a very weak (if any) dependence on temperature, inconsistent with one of the most recent measurements of the condensation coefficient.<sup>16</sup> This result implies that there exists a rate-limiting energetic or entropic barrier to evaporation. We note that previous experiments have shown that the velocity distribution of evaporating water molecules is Maxwellian,<sup>12</sup> which might indicate that the barrier to evaporation is entropic in nature. This may be due to possible geometric requirements for the evaporation of a water molecule.

**Acknowledgment.** This work was supported by the Chemical Sciences, Geosciences, and Biosciences Division of the U.S. Department of Energy. C.D.C. was supported by the National Defense Science and Engineering Graduate Fellowship and the ALS Doctoral Fellowship. We also acknowledge Kevin R. Wilson and Dick C. Co for early experimental work.

JA063579V

(36) Rudolf, R.; Vrtala, A.; Kulmala, M.; Vesala, T.; Viisanen, Y.; Wagner, P. E. *J. Aerosol Sci.* **2001**, *32*, 913.

(37) Laaksonen, A.; Vesala, T.; Kulmala, M.; Winkler, P. M.; Wagner, P. E. *Atmos. Chem. Phys.* **2005**, *5*, 461.